JOURNAL OF MECHANICAL ENGINEERING AND SCIENCES
ISSN: 2289-4659 e-ISSN: 2231-8380
VOLUME 19, ISSUE 2, 2025, 10653 - 10666
DOI: https://doi.org/10.15282/jmes.19.2.2025.7.0835

RESEARCH ARTICLE

Machine learning prediction of downstream oil carryover in air-oil separators for vacuum application

E. Nangi[1], F. Faraji[1]*, P. L. Chong[1], F. Hamad[1], L. Cochrane[2], J. Gonzalez[2]

[1] School of Computing, Engineering and Digital Technologies, Teesside University, TS1 3BX, Middlesbrough, UK
[2] PSI Global Limited, Stockton-on-Tees, TS22 5FE, Billingham, UK

ABSTRACT – Air or oil filters are commonly used in vacuum conditions in pumps within various industries such as healthcare, pharmaceutical, and many more. Some of these filters are exposed to an upstream challenge of 1000-20000 mg/m^3 of oil particles mixed with air, which needs to be reduced to 3-5 mg/m^3 downstream. Accurate determination of the carryover rate of oil by the filters is crucial for meeting environmental compliance and enhancing operational efficiency. Traditional methods for measuring the carryover rate rely on time-consuming and costly experiments, making them impractical for large-scale production and real-time quality assessment. Therefore, the main objective of this study is to develop digital models using mathematical and machine learning approaches to accurately predict the carryover rate in filters, thereby reducing reliance on physical testing. To this end, 224 sample experimental datasets were utilized, preprocessed, and cleaned to develop several multilayered Artificial Neural Networks (ANNs) and a multilinear regression model. Three optimisation strategies, including Levenberg-Marquardt, Bayesian Regularisation, and Particle Swarm Optimisation, have been used to tune the developed ANNs, which consist of various hidden layers and different neurons. For the purpose of comparison, the velocity-based physics model was applied to predict the oil carryover rate. The results of the study revealed that the single hidden layer with 20 neurons ANN optimized with the BR algorithm performed the best among all the models, with a Mean Square Error of 0.0648 and a correlation coefficient value of 0.942 for predicting the oil carryover rate. The developed model is validated and can be used for the fast computation of the carryover rate, informing the optimisation strategy of the filters.

ARTICLE HISTORY
Received : 18th Nov. 2024
Revised : 22nd Feb. 2025
Accepted : 03rd June 2025
Published : 30th June 2025

KEYWORDS
Air filter
Oil filter
Machine learning
Carryover rate
Vacuum pump

1. INTRODUCTION

In the post-pandemic era, there has been a surge in studies aimed at understanding the transportation of particulate matter and its impact on human health. Air pollution from particulate matter is the leading cause of cardiovascular diseases in developed and developing countries [1]. Industrial processes increasingly emit aerosols as by-products, which can vary in size and concentration depending on the upstream process [2]. Filtration is a scientifically designed technology that ensures high-quality air is released into the environment from various industrial processes. These separators typically have high porosity, usually above 70%, with a structure that allows for efficient microparticle separation and low flow resistance. Fibrous filters are used as the main component of aerosol separators because they are simple to operate, low-cost, and have a wide range of particle removal [3]. There is a relatively low pressure drop across these filters under diverse operating conditions. Filters are the key component in the filtration process. Therefore, the performance of these filters is carefully controlled to ensure compliance with various health and industrial standards. Aerosol separators find applications in various fields, including vacuum pumps and compressor cleaners, automotive booths, and respiratory protection systems. For instance, about 80% of the vacuum pumps in the industry are lubricated with oil mist. The filters in these pumps function to purify the exhaust air before it is released into the environment, ensuring safety. Additionally, they allow for the recovery of collected oil, which can be either reused or disposed of properly. The international health and safety executive guidance requires that the oil mist be reduced to 3 mg/m^3 [4]. This reduction in oil mist carryover from typically 1000−15000 mg/m^3 to 3mg/m^3 is known as the mass carryover rate. In the air-oil filtration industry, the performance of filters is tested according to ISO 29463; the mass carryover across the filter is the most important parameter. The concern is not only the filter's efficiency but also the size of the oil aerosol released by these industrial operations into the atmosphere. For instance, a filter that is 99% efficient, but with a carryover of 20 mg/m^3, from a challenge of 2000mg/m^3 is considered to be a faulty filter for this application as it will not pass the High-Efficiency Particulate Air (HEPA) filter regulation in the United States of America defined by the department of energy (MIL-STD-282) as 99.97%, the European standard (EN1822), and ASHRAE 52.2. A filter is considered optimal when it has a carryover to a challenge that results in an efficiency of 99.99% with low flow resistance, as defined by the pressure drop across the filter. The filtration efficiency is simply calculated as:

$$\text{Efficiency} = (\text{challenge} - \text{carryover})/\text{challenge} \quad (1)$$

*CORRESPONDING AUTHOR | F. Faraji | ✉ f.faraji@tees.ac.uk

Therefore, the accurate determination of the carryover rate in the filtration industry is crucial to meet the required regulations and optimize the performance of these separation media. The determination of such key parameters is typically performed through experimental methods, such as the Gravimetric Method (Filter Weight Gain), which measures the oil mass collected by a downstream filter over time. Other techniques include Laser Photometry, using light scattering to assess oil aerosol concentration, Condensation Nuclei Counters (CNC) for detecting ultra-fine mist particles, Gas Chromatography (GC) for analyzing the chemical composition of exhaust gases, and Isokinetic Sampling, which measures oil mist under dynamic airflow conditions using an isokinetic probe [5]. Each experimental method for measuring oil mist carryover has trade-offs between accuracy, cost, and practicality. While gravimetric analysis lacks real-time monitoring and struggles with ultra-fine mist, laser photometry and condensation nuclei counters require complex calibration and are sensitive to environmental factors. Gas chromatography provides precise chemical analysis but is time-consuming and expensive, whereas isokinetic sampling is highly accurate but requires a complex setup and skilled operation [6]. Additionally, it is not feasible or practical to carry out the measurements if a variety of filters with different sizes, dimensions, and lengths are available. Hence, a digital model that can accurately predict the carryover rate of the filters can be a valuable asset for engineers, saving costs and time while enabling faster system optimization and providing predictive insights, thereby ensuring efficient filtration and preventing failures [7]. Most of the modelling work in the literature for fibrous filters focuses on the efficiency of the filters for varying fibre arrangements, pressure drop across the filters, and CFD modelling of the various complex processes associated with fibrous filters [8]. Less attention is given to the practical modelling of carryover rate, which is the primary purpose of the filter design and operation. Additionally, the carryover rate is directly related to the performance and efficiency of the filters in numerous research studies. In this context, the study by [9] focuses on improving filtration performance while minimizing energy consumption in Heating, Ventilation, and Air Conditioning systems by looking at initial pressure drop and dust-holding capacity. They developed empirical models to predict filtration carryover performance based on factors such as fiber diameter, filtration velocity, pleat depth, and pleat density. The empirical models were validated using a full-scale air filter test experiment. Hubbard et al. [10] investigate the efficiency of fibrous filters in the viscous inertia transition flow regime by conducting low-pressure air experiments. They used normal distribution particle sizes of $2 - 1\mu m$ of sodium chloride and iron nano agglomerate as the aerosol. Leung and Hung [11] investigated the pressure drop and filtration efficiency under continuous loading of sub-micron aerosol particles in fibrous filters, and they developed a semi-empirical model to describe the pressure drop across a fibrous filter under continuous loading conditions. The performance of the various fibrous filters reviewed in the literature emphasizes the influence of the filter's inherent properties, such as fiber orientation, fiber width, porosity, and packing density, as well as the flow parameters, on the deposition of aerosol downstream [12]. In a production setting where the objective is to design filters with optimal performance for varying flow conditions and applications, it will be imperative to relate these factors. The fibrous molding parameters, such as injection pressure, fiber mix density, fiber width, and orientation, will provide invaluable information for such correlation. Dhaniyala and Liu [13] investigated the variation of packing density on the performance of nonuniform fibrous filters and emphasized the importance of filter inherent properties in determining filtration efficiency for detecting aerosols downstream.

Jackiewicz et al. [14] investigate the enhancement of aerosol particle filtration using nanofibrous media in fibrous filters. The research focuses on enhancing the initial filtration efficiency while maintaining a low pressure drop across the filter. The paper primarily addresses how the fiber diameter and filter porosity, crucial characteristics of the filter structure, impact filtration performance. The performance of these filters was evaluated based on two key metrics: initial pressure drop and filtration efficiency [14]. The study found that nanofibers significantly improve filtration efficiency without causing a prohibitive increase in pressure drop. By using fibers with diameters below 1 μm, the filter's performance was enhanced, particularly in capturing the most penetrating particle size (MPPS). Pan et al. [9] examines how the architecture of fibrous filters, particularly nanofibers, contributes to particle filtration and potential carryover issues. This simulation-based study provides insights into optimizing filter designs to minimise carryover. A well-accepted physics model for computing the carryover rate (particles from a fluid stream) of filters is known as the velocity-based carryover model, which is based on the amount of oil bypassing the filters. The various mechanisms influencing particle capture are accounted for, and the model can be presented as follows.

$$C = C_{inlet} \times (\mathrm{e}^{-\eta} + kV^n) \tag{2}$$

where, C represents the Predicted Carryover Rate (mg/m³), C_{inlet} The inlet concentration model can be calculated based on the flow rate, Q, as aQ^b, a and b are optimisation parameters. kV^n is the correction term based on velocity, V to adjust the turbulence in the flow, where k and n are optimisation constants. The filtration efficiency, η was computed using the standard filtration efficiency model equation as:

$$\eta = 1 - e^{-\left(\frac{QL}{\rho D}\right)} \tag{3}$$

where Q is the flow rate in (m^3/s), L is the filter length in meters, ρ is the fluid density in kg/m^3, and D is the filter diameter in meters. The power of the exponent, also known as the filtration coefficient, β, is influenced by three mechanisms of inertial impaction, interception, and diffusion. Larger particles deviate from airflow streamlines and collide with filter fibres due to inertia, while medium-sized particles follow the airflow but contact fibres through interception. On the other hand, smaller particles undergo random motion due to gas molecule collisions, increasing their chance of striking a fibre through diffusion [15]. Although physics-based models provide valuable insights into filtration behavior, the assumption

of a uniform particle distribution, steady-state flow, and idealized fiber geometry would oversimplify the approach, which might lead to unexpected errors [16].

In recent years, soft computing and data-driven approaches have been applied to modelling and predicting filter performance. Piotrowski and Napiorkowski [17] developed a hybrid model using Gradient Boosted Regression Tree (GBRT) and differential evolution (DE) to predict pressure drops in sand filters used in micro-irrigation systems. Balcilar et al. [18] employed an ANN model to classify filter sizes and predict differential pressure across a filter. Beckman et al. [19] discuss the various analytical approaches for predicting air filtration efficiency and air flow resistance, including the Single Fibre Efficiency Theory (SFE). They used artificial simulated media and a convolutional neural network (CNN) to predict the performance of a filter based on SEM images. To this end, no study has correlated key process parameters for the reliable modeling of carryover rate using any soft computing approaches, such as machine learning. In this study, ten process parameters were correlated with the oil carry-over rate downstream, and practical models to predict this important parameter have been developed.

2. MATERIALS AND METHODS

The method used in this work involves a well-designed experiment of the moulding process that produces the filter. This is followed by porosity testing to determine the filter's porosity and permeability. The produced filters are then tested in an application test experiment. The development of numerical modelling follows this via machine learning to correlate the production process to the carryover rate of oil mist downstream. The developed model can be used to predict the performance of filters with varying moulding parameters. The filter production process is illustrated in Figure 1, where in Stage A, fibre filters are produced using the injection moulding process. The produced filters are shown in Figure 1(b), and they are impregnated with resin in Figure 1(c).

(a) (b) (c)

Figure 1. Fibrous filter moulding process: (a) Injection rig, (b) Moulded tube, and (c) Resin impregnation

2.1 Experimental Setup

Injection moulding is the manufacturing process used to produce the fibrous filters used in this study. This is a flow-forming process at high pressure where both fibres and polymers exhibit bulk flow [1]. It is one of the most widely used methods in the production of plastics and reinforced fibrous parts. The fibrous filters used in this study are made from borosilicate glass fibre. The fiberglass of known fiber properties is weighed on a balance and mixed in a slurry tank to obtain a predetermined composition. Highly concentrated acid is added to the mixture to maintain its acidity. The weight of the fibreglass per unit of water is measured and recorded, as well as the pH of the mixture. The mixed slurry is passed to a moulding tank and pumped through a patented moulding technology to mould the fibrous tube in a moulding rig. The moulding process is controlled by the pressure with which the slurry is injected into the rig. This pressure is referred to as the moulding or injection pressure. The moulded tube is impregnated with an acrylic binder for better structural rigidity. The impregnated tube is then cured in an oven to obtain a dry moulded tube. The process is well-controlled to ensure uniformity in the production of filters for different batches. The fibre width is controlled by ensuring that fibre glass with predetermined properties is used.

The experiments in this paper were conducted using the test rig at the PSI Global Limited laboratory. Figure 2 shows the setup of the test rig designed to measure the oil carryover downstream of the air/oil separator. The rig consists of a vacuum pump with a test chamber. The moulded fibrous filter is fitted to the vacuum chamber during testing. The instrumentation part of the rig consists of a flow meter to measure the flow rate of the fluid that is introduced to the test chamber. A vacuum pressure manometer and thermometer are used to measure the vacuum pressure and the temperature in the vacuum. The differential pressure gauge measures the pressure drop across the filter, and the dust tract aerosol photometer records the aerosol carryover at the exhaust. The vacuum pump is loaded with the manufacturer's recommended mineral oil. The experiment is started by saturating a fibrous filter in the testing chamber of the vacuum pump. This saturation process is necessary to simulate the filter's operation at maximum saturation with oil. A mixture of air and suspended particles of mineral oil is introduced into the testing chamber. The typical challenge going into the filter

ranges from 1000 to 15000 mg/m³, depending on the size of the vacuum pump. However, for the vacuum pump used in this experiment, the challenge is 3574 mg/m^3. The measuring instruments are switched on at the end of the saturation process, and the oil carryover, as well as the flow, vacuum, and operating parameters, are recorded. A gravimetric study is used to benchmark the values of carryover recorded by the photometer according to ISO 29463. Filtration efficiency is a key indicator of filter performance. The filter efficiency measures the filter's ability to remove particles from a fluid effectively. A highly efficient filter has very low carryover, as most of the particles have been successfully removed by the filter. The efficiency and carryover are inversely related. To calculate the efficiency of the filter, the challenge, which is the mass of oil entrained by the gas, is correlated with the mass of entrained oil after filtration. In this experiment, the carryover of oil aerosol after the filtration is measured using the duct track aerosol photometer, as shown in Figure 2.

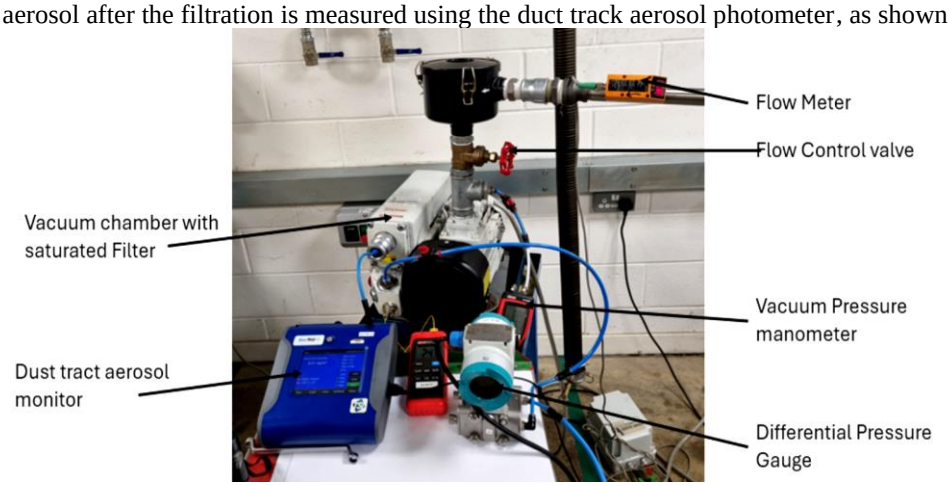

Figure 2. Fibrous filter testing developed rig in PSI Global

2.2 Variables and Data Preparation

The study takes into account both the fibrous tube moulding parameters and the testing quality parameters. The three process parameters that control the characteristics of the moulded filters are the injection pressure of the moulding rig, slurry pH, and the pad weight, which represents the mass of fibre per unit volume of water in the slurry tank. The injection pressure and pad weight represent the packing density and porosity of the fibrous filters. The end-test differential pressure and end-test efficiency are quality control parameters. The vacuum pressure, flow rate, differential pressure, and exit velocity are test parameters, and the carryover is a response parameter. Table 1 presents the collected parameters obtained during the experimental measurements for one of the filter samples. The experiment was conducted with various test samples, resulting in 224 data points collected. The details of the statistical analysis of the data in Table 2 indicate that the data cover a wide range, ensuring the comprehensiveness of the experimental data. The data is pre-processed and cleaned to remove empty cells and outliers using the *Z* score, with a standard quartile of -3 and 3 [20].

$$Z = \frac{X - \mu}{\sigma} \tag{4}$$

where *Z* indicates the number of experimental data points *that* deviate from the mean, μ, and σ is the standard deviation of the data set. A value with a Z-score greater than +3 or less than -3 is considered an outlier. After applying the method, two data points that fell outside the acceptable range were removed, and the cleaned dataset was used for analysis and modelling. The visual representation of the distribution of the Carryover rate (mg/m³) data is presented in Figure 3. The graph indicates that the majority of the data falls below the normal distribution line, making it suitable for developing a data-driven approach.

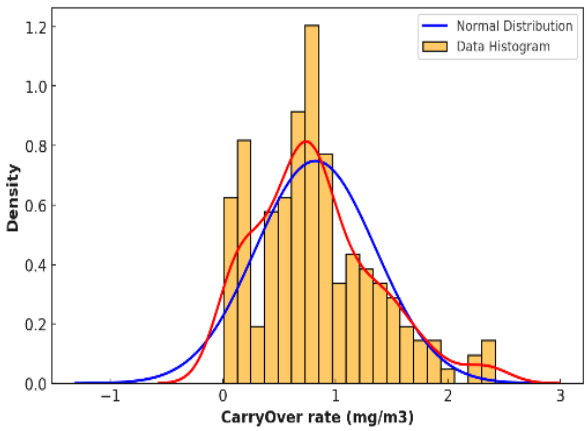

Figure 3. The distribution of the carryover rate in the collected experimental data

The impact and relevance of each collected variable are determined. In this work, the Pearson rank correlation coefficient is shown in Eq. (5).

$$r_{xy} = \frac{\sum_{i=1}^{n}(x_i - \bar{x})(y_i - \bar{y})}{\sqrt{\sum_{i=1}^{n}(x_i - \bar{x})^2}\sqrt{\sum_{i=1}^{n}(y_i - \bar{y})^2}} \quad (5)$$

where n is the sample size, 224 samples collected from the experiments, x_i and y_i are the individual sample points indexed with i, and $\bar{x}$ and $\bar{y}$ are sample mean values. To detect outliers in the data, the z-score method, with an absolute threshold, has been employed. The z-score method standardizes the variable by subtracting its mean and then dividing by its standard deviation.

Table 1. Sample example of the collected data for one filter

Sample number	Inverter Freq (Hz)	Pad Weight (g)	pH	Injection Pressure (bar)	Dp end test (mbar)	End Test Efficiency	$P_{Vaccume}$ (mbar)	Flow (Nm^3/h)	Vexit (m/s)	Dp (mbar)	Carryover rate (mg/m^3)
6973-19	50	6.3	2.98	3.44	86	0.0007	1019	0.0	0.010	4.4	0.012
	50	6.3	2.98	3.44	86	0.0007	950	6.5	0.036	69.0	2.000
	50	6.3	2.98	3.44	86	0.0007	900	9.5	0.053	88.0	1.750
	50	6.3	2.98	3.44	86	0.0007	800	19.0	0.110	122.2	1.740
	50	6.3	2.98	3.44	86	0.0007	700	26.3	0.150	158.5	1.750
	50	6.3	2.98	3.44	86	0.0007	600	38.9	0.220	194.9	1.640
	50	6.3	2.98	3.44	86	0.0007	300	76.0	0.420	300.3	1.300
	50	6.3	2.98	3.44	86	0.0007	35	112.4	0.620	393.1	0.840

Table 2. Statistical description of the experimental data

Statistical metrics	Inverter Freq (Hz)	Pad Weight (g)	pH	Injection Pressure (bar)	Dp end test (mbar)	End Test Efficiency	$P_{Vaccume}$ (mbar)	Flow (Nm^3/h)	Vexit (m/s)	Dp (mbar)	Carryover rate (mg/m^3)
Mean	46.8	5.65	3.07	1.74	68.83	0.00039	657	16.50	0.076	122	0.94
Median	47.5	5.50	3.10	1.57	69.00	0.0004	700	6.10	0.019	105	0.84
Mode	45.0	5.50	3.10	0.83	63.00	0.0005	900	0.00	0.000	125	1.31
Standard Deviation	1.97	0.25	0.047	0.72	5.75	0.0002	321	25.00	0.150	91.2	0.61
Kurtosis	-1.23	1.62	-1.13	-0.2	1.13	-0.104	-0.52	6.89	7.560	0.019	0.82
Skewness	0.48	1.68	-0.83	0.54	1.04	0.35	-0.86	2.67	2.840	0.75	0.81
Minimum	45	5.50	2.98	0.60	60	0.00	10	0	0.000	0.04	0.007
Maximum	50	6.30	3.10	3.44	86	0.0008	1020	123	0.680	393	3.34

2.3 Machine Learning Models

Among the many machine learning (ML) models available in the literature, this study adopts MLR and Multi-Layered Artificial Neural Networks (MLANN) for predicting the carryover rate in porous filters. MLR is a well-established statistical method that provides clear insights into the relationship between predictor variables and the response variable (carryover rate). Additionally, it is computationally efficient, requiring fewer data points compared to more complex ML algorithms such as Random Forest (RF) or Support Vector Machines (SVM). Moreover, MLR expresses the relationship between input parameters and the output (carryover rate) in the form of a linear correlation, making it easy to interpret and understand. On the other hand, MLANN can capture nonlinear relationships, which are expected in a fluid filtration system where multiple variables interact in a complex manner. The model is particularly suitable for optimizing the carryover rate, as it can learn hidden patterns in the data, thereby enhancing predictive accuracy. Both MLR and MLANN have been successfully applied in previous studies, such as in predicting hydraulic conductivity in porous soils [21] and in modeling flow interactions in highly porous hydrocarbon reservoirs [22]. Their demonstrated effectiveness in similar domains justifies their selection for this study. In multiple linear regression, the response variable is predicted by several predictor variables. In this work, the average oil carryover in mg/m^3 is predicted to the mixture pad-weight (g), inverter frequency (Hz), pH, injection pressure, end test differential pressure (mbar), end test efficiency, vacuum pressure (mbar),

flow rate (Nm^3/h), and the differential pressure (mbar). The equation produced from the regression modelling is of the form:

$$Y_{CO} = K_1X_{1F} + K_2X_{PH} + K_3X_{1P} + K_4X_{EDP} + K_5X_{ETE} + K_6X_{VP} + K_7X_F \quad (6)$$

where X_n is the corresponding prediction parameters, $K_{1\text{-}n}$ are the constants of the equation and Y_{CO} is the predicted output carryover downstream of the separator. Another model utilized in this study is artificial neural networks. ANNs are a form of artificial intelligence, highly nonlinear approximators that mimic the nervous system in the human body. These networks can learn, store, and recall information, functioning as massively parallel distributors. ANNs are recognized for their generalization capability, adaptability to learning, and ability to handle large amounts of information. Additionally, ANNs excel at modelling data with highly nonlinear relationships between variables. Unlike other algorithms, such as decision trees, ANNs tend to perform better if sufficient data is provided during the training phase. The most popular type of neural network is the multilayer perceptron (MLP), which consists of several layers, including an input layer, a hidden layer, and an output layer. Typically, a single hidden layer in an MLP is sufficient for generalising most problems. For more complex problems, additional layers with varying numbers of neurons can be added to enhance accuracy. Layers are connected by links known as weights, which are numeric values that define the strength or weakness of these connections. The output of each layer is determined by combining the weighted sum of the inputs and a bias value. Once this output is computed, it is processed through an activation function before being passed to the next layer. The activation function establishes a mathematical connection between the input and output, commonly taking forms such as linear, sigmoid, or hyperbolic tangent functions, as shown in Equation 6. These functions play a crucial role in defining the behaviour and transformation of the data as it flows through the network.

$$\begin{cases} \text{Linear} = f(x) = x \\ \text{Sigmoid} = f(x) = \dfrac{1}{1+e^{-x}} \\ \text{Sinusid} = f(x) = \sin(x) \\ \text{Tansig} = f(x) = \dfrac{2}{1+e^{-2x}} - 1 \\ \text{Arctan} = f(x) = tan^{-1}(x) \end{cases} \quad (7)$$

The mathematical representation of an MLP network, comprised of one hidden layer with a sigmoid function, is shown in Eq. (8).

$$\text{Output} = \text{purelin}\,(w_2 \times (\text{sigmoid}(xw_1 + b_1) + b_2)) \quad (8)$$

where b_1 and b_2 are biases, and w_1 and w_2 are the weight matrices for the middle and output layers, respectively. The learning process in an ANN involves adjusting the weights and biases to establish a relationship between the predicted and desired outputs [23-29]. Initially, the trained model may be highly unstable and perform poorly due to incorrect values of weights and biases [30]. Throughout the learning process, the weights and biases are updated with each iteration, reducing the cost function until the satisfactory criteria are reached. After constructing the model and determining the number of neurons in the hidden layer, initial training is conducted using specific training algorithms, and the model is then optimized using specific optimization algorithms. In this study, we initially constructed an ANN topology, illustrated in Figure 4, for predicting the oil carryover rate in the filters.

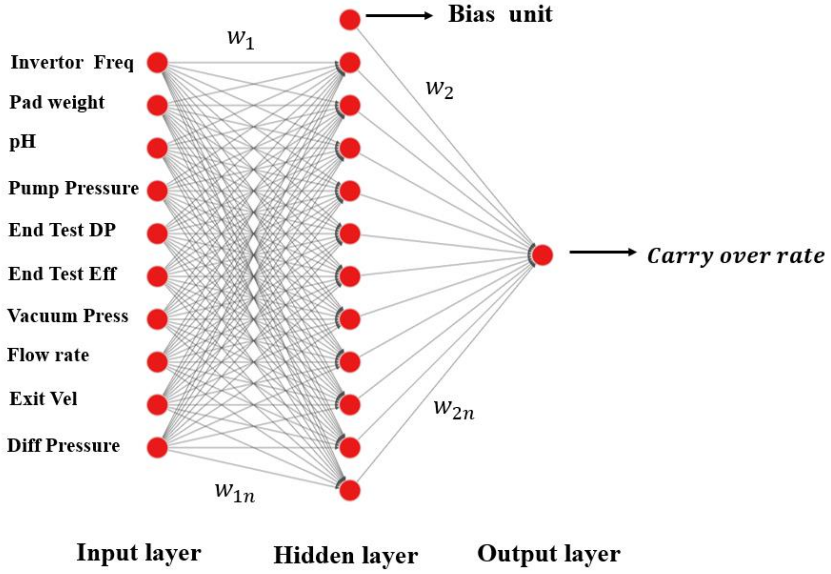

Figure 4. The proposed multilayer neural network to predict the carryover rate

In the developed ANN topology, the first layer, referred to as the input layer, corresponds to the input data. The middle layer is the brain of the network, where the computations are performed, and the last layer generates the network's output.

An MLP with one hidden layer is generally capable of handling a wide range of problems with sufficient accuracy. However, in cases where enhanced performance is needed, adding more hidden layers can be beneficial [31, 32]. The number of hidden layers and neurons required is highly dependent on the problem's complexity, and these values are often determined through empirical methods [33]. This study identified the optimal MLP structure, including the configuration of hidden layers and neuron counts, using a trial-and-error strategy.

2.4 Optimisation Mechanisms

2.4.1 Levenberg–Marquardt algorithm

The Levenberg–Marquardt (LM) algorithm is one of the most commonly used optimisation techniques for calculating weights and biases in neural network architectures [26, 34]. Originally introduced by [35], the LM algorithm is renowned for its fast convergence and superior performance in establishing relationships between input and output variables compared to traditional gradient descent methods. The network performance is determined through the sum of the squared errors, and the Hessian matrix can be calculated as follows.

$$\begin{cases} H = J^T J \\ g = J^T e \end{cases} \tag{9}$$

In this context, J represents the Jacobian matrix, which consists of the first-order derivatives of the network's error to the weights and biases, e is an error vector, and H is the Hessian matrix. The LM algorithm uses this approximation to establish the relationship between the network's input and output variables, and it updates the weights in each iteration accordingly.

$$W_{k+1} = W_k - \left[{J^T}_{W_k} J_{W_k} - \mu I \right]^{-1} \times {J^T}_{W_k} e_{W_k} \tag{10}$$

where W denotes the network's weights during the $k+1^{th}$ and k^{th} iterations. Here, I refer to the identity matrix, while μ acts as a damping parameter or stabilizing constant. The key distinction between the LM method and the Gauss-Newton approach lies in this stabilizer, which allows the LM algorithm to adapt its search strategy [36]. A comparative analysis by [17] found that the LM algorithm surpassed eight other evolutionary algorithms in training artificial neural networks.

2.4.2 Bayesian-Regularization algorithm

The minimization of the cost function in an MLP neural network using the Levenberg–Marquardt algorithm is achieved through the backpropagation method. This involves minimizing the sum of squared errors through an iterative process with a defined stopping criterion. This criterion is determined using a validation dataset that is not involved in the development of the trained model [37]. The iteration process is halted when the squared error for the validation dataset reaches its minimum. Continuing training beyond this point would result in overfitting the model, leading to increased squared error and reduced accuracy. Additionally, the validation dataset is selected randomly, and repeating the entire computational procedure can lead to overfitting [14]. To address this issue, [30] proposed the Bayesian-Regularization algorithm for neural networks, which does not require a validation dataset. Instead, this method incorporates Bayes' theorem into the regularization scheme by adding two additional hyperparameters (β and α) to the cost function, S_w, as follows.

$$S_w = \beta \sum_{i=1}^{N_D} [y_i - f(X_i)]^2 + \alpha \sum_{j=1}^{N_w} {w_j}^2 \tag{11}$$

where N_W represents the number of weights, y_i is the number of experimental data, and $f(X_i)$ is the model's output within the matrix of N_D. The weight matrix for the training dataset is indicated by w_j. Random numbers between the range of $0<\alpha<10$ and $100<\beta<500$ for the hyperparameters α and β. As the iterations progress, these values are optimized to minimize the cost function effectively.

2.4.3 Particle swarm optimization

Inspired by the natural behaviours of swarming and flocking seen in birds, fish, and insects, an evolutionary algorithm called Particle Swarm Optimization (PSO) was introduced by [38]. A common analogy to illustrate the core concept of PSO is the way a flock of birds searches for food. Although none of the birds know the exact location of the food, they are all generally aware of its approximate distance. Initially, they move toward the food source at random speeds, but over time, based on their own flying experiences and observations of other birds, they start following those closest to the food. This process continues, with the group gradually updating their positions until they successfully find the food source. In PSO, the fitness function measures the distance between the birds and the food. The algorithm begins with a set of random solutions, referred to as particles, which are distributed throughout the search space. Each particle has a random velocity and position. In each iteration of the optimization process, the fitness function is applied to assess the fitness of each particle [39]. The best position that each particle has visited, referred to as the personal best (pbest), is identified, as well as the global best (gbest), which is the best position achieved by the entire swarm. The velocity, V and position, X, of each particle are updated using two specific equations to adjust their movement through the search space. This iterative process continues until the particles converge on an optimal solution.

$$\begin{cases} V_i(t+1) = w.V_i(t) + c_1.rand_1.\left(pbest_i(t) - x_i(t)\right) + c_2.rand_2\left(gbest_i(t) - x_i(t)\right) \\ X(t+1) = X_i(t) + V_i(t+1) \qquad (i = 1 \ldots . N) \end{cases} \tag{12}$$

where V_i represents the initial velocities (from the previous iteration "t"), while t=1 indicates the new velocities. The term w denotes the inertia weight for each particle within a population of N particles. The constants c_1 and c_2 are learning factors that define the relative influence of cognitive and social components. The cognitive term reflects the particle's individual experience, while the social term captures the collaboration among particles (a collective effort). To begin the iterations, two random numbers ($rand_1$ and $rand_2$) are introduced, both ranging between 0 and 1. The algorithm's exploration efficiency is evaluated using an updated weight function, and the optimal weights are determined by employing a global minimum search mechanism.

3. RESULTS AND DISCUSSION

3.1 Effectiveness of the Coalescing Filters

The above-explained machine learning models have been applied to predict the performance of air/oil separators in vacuum applications in terms of the remaining oil downstream (carryover). In addition, a physics-based model known as the Velocity-Based Model is also applied to the same task. The effectiveness of coalescing filters in oil removal is defined according to ISO 12500. Figure 5 shows the performance of the moulded tubes from the application test experiment of section 2. The coalescing separators studied in this work all exhibit a very high oil removal rate. These are considered highly optimal air/oil separators, as per ISO 12500, with an efficiency above 99.995%. Figure 5 shows the oil carryover downstream at varying air velocities for four different separators with injection pressures ranging from 0.6 to 3.44 bar. At each of the tubes, the carryover is maximum when the flow velocity is less than 2, and decreases continuously as the flow velocity increases. This is consistent with the vacuum pump operating principles; as the flow velocity increases, the mass concentration of the aerosol within the air decreases. Additionally, the increased flow velocity increases the Reynolds number, which in turn ensures the reduction of oil aerosol from settling accordingly. Figure 5 also illustrates the effect of injection pressure on oil carryover. Higher injection pressure will mean the fiber materials are closely packed together, limiting the pore spaces. In addition, due to the effect of using a binder to hold these fibers tightly together, the more pore spaces in the low-injection-pressure region, the more likely they are to be filled by the binder, leading to low-porosity media. This would ultimately affect the carryover rate, and understanding the right balance between injection pressure and other moulding parameters to produce more effective separators will require models that correlate the input parameters with the output (carryover rate).

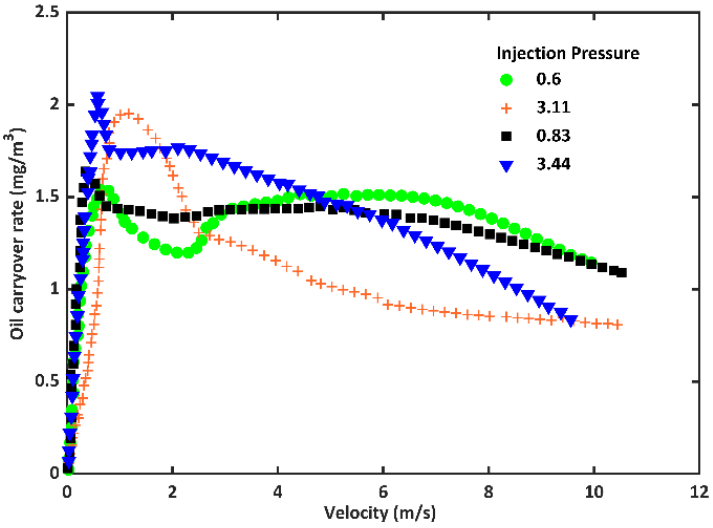

Figure 5. Performance of moulded coalescing filters

3.2 Proposed Carryover Rate Models

To predict oil carryover downstream, an MLR model and an ANN were developed. The proposed MLR model is expressed as:

$$carryover\ rate = -60 - 0.524XIP + 12.52XpH + 4.10XPW + 0.000280XV - 0.00216XF) \tag{13}$$

where XIP, XpH, XPW, XV, and XF are inlet pressure, pH of the fibre glass solution, pad weight, exit velocity, and inventor frequency, respectively. The coefficient of determination, R^2 = 0.8312, and MSE = 0.13185, indicate that the MLR model captures most of the variance in the dataset but may struggle with nonlinear relationships. To assess model reliability, an Analysis of Variance (ANOVA) was conducted, and the results are presented in Table 3.

Table 3. The results of the ANOVA analysis of the input variables

Source	DF	Adj SS	Adj MS	F-Value	P-Value
Regression	5	12.3618	2.47237	25.87	0.000
Injection Pressure (Bar)	1	0.4022	0.40216	4.21	0.043
pH	1	0.2205	0.22053	2.31	0.133
Pad Weight (g)	1	0.5480	0.54804	5.73	0.019
Vacuum (mbar)	1	0.1681	0.16807	1.76	0.188
Flow (Nm^3/h)	1	0.1006	0.10063	1.05	0.308
Error	1	7.9326	0.09557	-	-
Lack of fit	1	7.8782	0.09608	1.76	0.546
Pure Error	83	0.0545	0.05445	-	-
Total	88	20.2945		-	-

The result of the ANOVA provides a comprehensive breakdown of the sources of variation in the dataset, allowing us to assess the significance of different predictors on the response variable. This discussion will interpret the key components of the ANOVA and their implications for the study. The F-value represents the overall significance of the model in the ANOVA, where a higher F-value indicates that the model explains a significant amount of the variance in the data. On the other hand, a p-value of the ANOVA indicates whether the observed results are statistically significant. If the p-value is less than 0.05, it suggests that the models' inputs have a statistically significant impact on the output variable. The regression model is statistically significant ($F = 25.87$, $p < 0.001$), meaning the predictors collectively influence oil carryover. This indicates that the predictors collectively explain a significant portion of the variation in the response variable. The injection pressure has an F-value of 4.21 and a p-value of 0.043, indicating that it is statistically significant at the 5% level. This suggests that variations in injection pressure have a meaningful impact on the response variable (oil carryover). On the other hand, the pH, with an F-value of 2.31 and a p-value of 0.133, is not statistically significant at the 5% level of significance. This implies that pH variations do not significantly affect the response variable in this model. In addition, the pad weight (g), with an F-value of 5.73 and a p-value of 0.019, showed that it makes an important contribution to the developed models. Moreover, both vacuum pressure (mbar), with an F-value of 1.76 and a p-value of 0.188, and flow rate (Nm/h), with an F-value of 1.05 and a p-value of 0.308, show that they are statistically insignificant for the model. The error term, with a sum of squares of 7.9326 and a mean square of 0.09557, represents the variation not explained by the model. The lack-of-fit test, with an F-value of 1.76 and a p-value of 0.546, is not significant, indicating that the model fits the experimental data well and that the residual variation is primarily due to random error rather than poor model performance.

The result of ANOVA suggests that there is no obvious heteroscedasticity (non-constant variance) in the model's errors, indicating that the assumption of constant variance is met. The ANOVA (Table 3) collectively suggests that the assumptions of normality, constant variance, and independence of errors are reasonably met, with minor concerns about potential outliers. The significant predictors, injection pressure and pad weight, should be considered critical factors in the study, as they have a meaningful impact on the response variable. The non-significant predictors, while not influential in this model, may still be relevant in other contexts or with different datasets. This statistical analysis aligns with the Pearson correlation results (Figure 6), confirming that injection pressure and pad weight should be prioritized in filter optimisation and for practical prediction of the carryover rate. Additionally, this suggests that any future physics-based models for predicting oil mist carryover should consider pad weight and injection pressure as two key parameters, as they have a significant impact on the accuracy and reliability of the prediction. The other variables are essential in the production and performance of these moulded fibrous filters. Therefore, more robust models are required that can predict oil carryover by relating production to performance parameters.

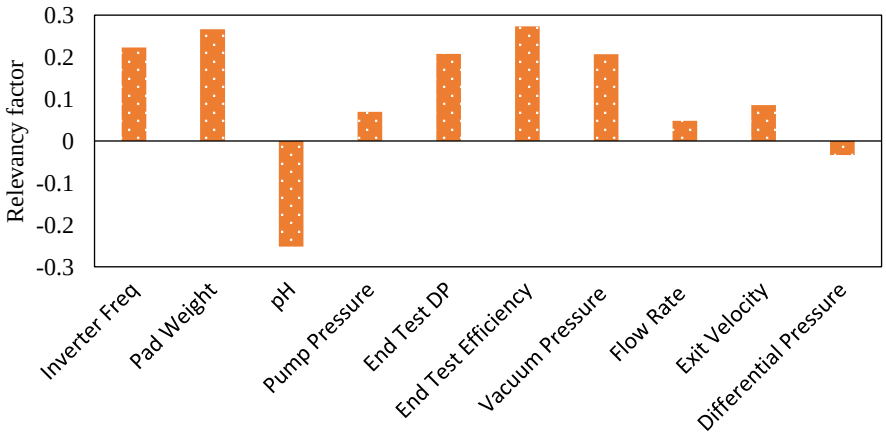

Figure 6. The impact of the input variable in the experiments on the carryover rate

To develop a robust model that captures nonlinearity in the database, an MLANN topology based on feed-forward neural networks was created. The network was tuned by varying the number of hidden layers and the number of neurons in each layer. A trial-and-error approach was employed for this purpose. As a result, a total of 120 neural networks were developed: 60 networks optimized using the LM algorithm and 60 optimized using Bayesian Regularization (BR). The performance of these networks was assessed using the statistical parameter of Mean Squared Error (MSE) across the training, validation, and testing stages.

Hence, to ensure the robustness of the ANN models, a systematic validation process was followed. Before training, the dataset was pre-processed by normalizing input features and splitting the data into training, validation, and testing sets. This approach ensures that the models generalize well and prevent overfitting. The testing errors were compared to select the best models among the developed networks, following the guidelines of [40] and [28]. This process, known as cross-validation, was used to assess the networks' generalization ability on unseen data. Based on the validation set's MSE, the best architectures were identified as 10–20–1 and 10–35–1 for the LM and BR algorithms, respectively. In this architecture, the first number represents the input nodes, the second represents the neurons in the first hidden layer, and the last indicates the output nodes. The networks with one hidden layer performed the best for the dataset used in this study. This validation methodology strengthens the credibility of our findings by ensuring that the selected models were rigorously evaluated before deployment. For the data utilised in this study, the networks with one hidden layer performed the best. The graphs in Figure 7 illustrate the performance of the feedforward neural networks constructed using the LM and BR algorithms. Two statistical parameters, the mean square error and the coefficient of determination (R), *were* utilised to assess the performance of the developed models. MSE quantifies the average squared differences between the predicted and actual carryover rates, where a lower MSE indicates better model accuracy. The coefficient of determination measures how well the model explains the variability in the data. A value close to 1 means strong predictive ability, while a lower value suggests poor correlation.

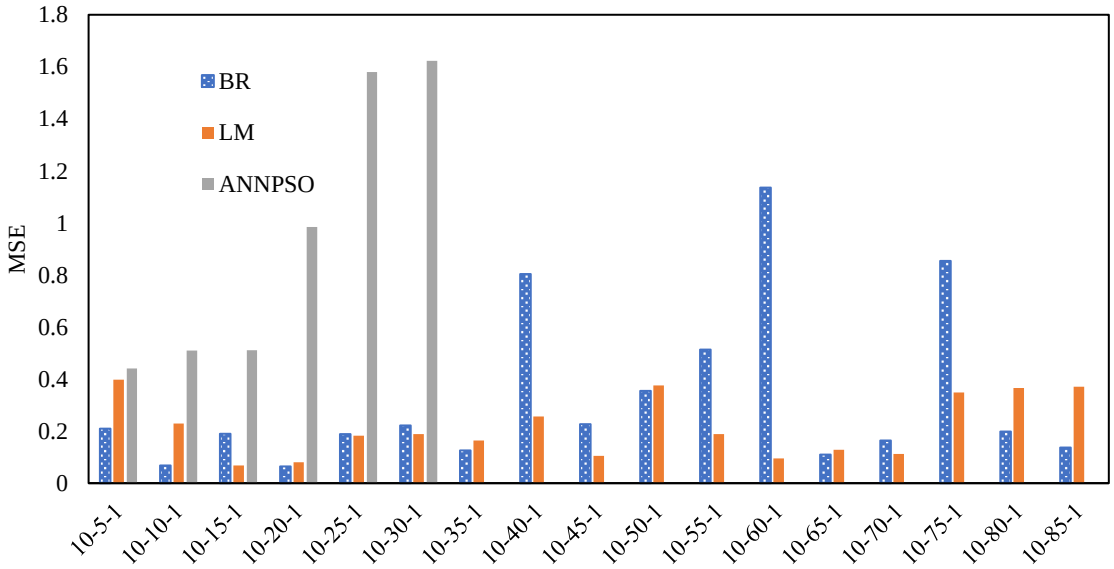

Figure 7. The performance of feed-forward neural networks in terms of MSE

Table 4. The statistical performance of the developed models in predicting the carryover rate of the filters

Model	MSE	R
ANN – PSO (10-5-1)	0.1954	0.671
ANN – LM (10-15-1)	0.0685	0.869
ANN – BR (10-20-1)	0.0648	0.942
Multiple regression model	0.1319	0.831
Velocity Based model (VBM)	0.2593	0.537

Table 4 shows the performance of each model in terms of MSE and *R*. The results show that the network with a 10–20–1 (BR) structure has the best performance among all, with the lowest MSE of 0.0664. Particle swarm optimisation was applied to optimise further the ANN that had been developed. This was applied to the different architectures, starting with the 10-5-1. However, the mean square error continued to increase as the number of neurons increased. The PSO optimisation of the ANN was therefore stopped when the mean squared error increased from 0.44 to 1.68. The PSO algorithm exhibits sub-optimal performance for this application, achieving a correlation coefficient R of 0.671. In contrast, the Artificial Neural Network with Bayesian Regularisation (ANN-BR) demonstrates superior regression accuracy, with a correlation coefficient of 0.942 and MSE of 0.0664. PSO is a population-based optimization algorithm that excels in finding global optima in complex search spaces. However, it may struggle with convergence speed and precision in regression tasks, especially when the problem space is highly nonlinear. The PSO is based on particle movement across

the search space, which makes it inefficient for file tuning, and it can also become stuck in local minima. The ANN-BR, on the other hand, is designed explicitly for regression tasks and it optimises model weights in a way that balances complexity and accuracy. The BR helps prevent overfitting by incorporating regularization terms in the cost function, leading to better generalization and more accurate predictions. Neural networks, particularly those with Bayesian Regularization, are adept at modelling complex, nonlinear relationships due to their ability to learn from data and adjust weights accordingly.

The performance of the best ML model (ANN-BR) was compared to the well-established Velocity-Based Model (VBM), a physics-based approach. Both statistical (Table 4) and graphical (Figure 8) error analyses demonstrated that the ANN-BR model outperforms the physics-based model, achieving greater accuracy and reliability. The problem addressed in this work is inherently nonlinear, as the process, testing, and performance parameters do not exhibit a direct linear relationship. For instance, the pad weight and the injection pressure, which are the two process parameters that essentially control the packing density and porosity of the fibrous filters, could proffer varying design and performance scenarios for the moulded tubes. Other parameters, such as the capillary effect and the rate of oil imbibition of the aerosol particles across the tubes, as well as permeability, depend closely on the flow rate and vacuum pressure upstream of the tube. Considering these factors individually could lead to the duplication of experimental tests that are not the focus of this work. However, the pad weight and injection pressure have controlled the tube porosity and permeability. An application test experiment has been designed to test varying operating flow conditions, ranging from when the vacuum pump is closed to when it is fully open. This way, the experimental design is robust and captures both the process parameters and the performance parameters. To ensure the validity of our regression models, we tested the assumptions of normality, constant variance (homoscedasticity), and independence of errors using both graphical and statistical methods.

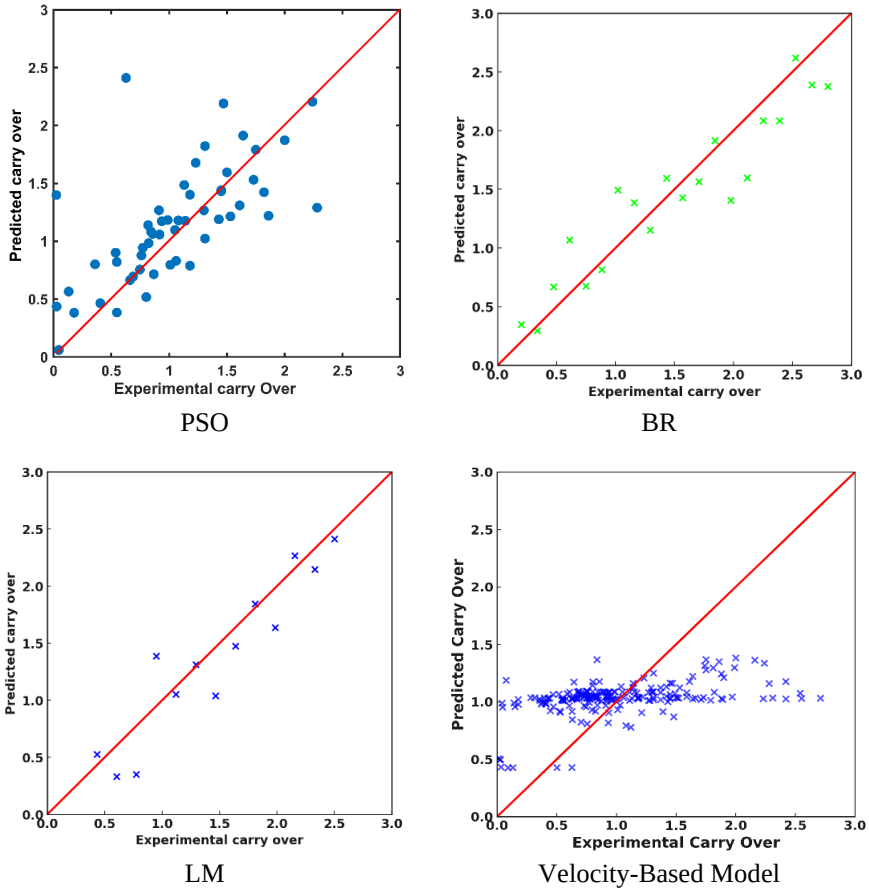

Figure 8. The performance of the developed ANN optimized by PSO, LM, and BR

4. CONCLUSIONS

In this study, the carryover rate, which refers to the remaining oil downstream in porous separators (filters) and serves as a critical performance indicator, was modelled as a function of nine moulding parameters. A dataset of 224 experimental observations was utilized to develop machine learning-based predictive models, including a multilayer ANN and a multi-linear regression model. To optimize the ANN architecture, different optimization algorithms, such as LM, BR, and PSO, were applied across various hidden layer configurations. A total of 120 multilayer neural networks were trained and evaluated. The best-performing network, as determined by the lowest MSE and highest R-value (correlation coefficient), was identified as ANN-BR (10-20-1). The predictive accuracy of the proposed ANN-BR model was compared with that of both the multilinear regression model and the velocity-based model. The results demonstrated that

ANN-BR significantly outperformed all other models, achieving the lowest MSE of 0.0648 and the highest R-value of 0.942, confirming its reliability in predicting the downstream oil carryover rate in filters. These machine-learning models can be directly implemented as predictive tools to replicate time-consuming and costly filtration experiments. This study offers valuable insights for process engineers seeking to optimize the performance of molded air/oil separators and enhance existing manufacturing processes through the application of machine learning techniques. Additionally, these models can be used to dynamically fine-tune process parameters, ensuring compliance with evolving industry standards and enhancing overall operational efficiency.

ACKNOWLEDGEMENTS

We would like to acknowledge the PSI Global Ltd engineering team for providing the lab facility used for the data acquisition of the project. The UKRI Innovation supported this work as part of the Knowledge Transfer Partnership (KTP) between Teesside University and PSI Global (Grant No. 11625063).

CONFLICT OF INTEREST

The authors declare that they have no conflicts of interest.

AUTHORS CONTRIBUTION

E. Nangi (Methodology, Conceptualization; Investigation; Formal analysis; Writing - original draft; Software; Investigation)

F. Faraji (Methodology; Data curation; Writing - review & editing; Formal analysis; Software; Investigation; Funding acquisition; Supervision)

P. L. Chong (Writing - review & editing; Visualisation; Supervision)

F. Hamad (Supervision; Writing - review & editing)

L. Cochrane (Methodology; Formal analysis; Resources)

J. Gonzales (Methodology; Formal analysis; Resources)

AVAILABILITY OF DATA AND MATERIALS

The data supporting this study's findings are available on reasonable request from the corresponding author.

ETHICS STATEMENT

Not applicable**.**

REFERENCES

[1] N. Reynolds, M. Pharaoh. An Introduction to Composites Recycling. 1st Ed. United Kingdom: Woodhead Publishing, 2010.

[2] Z. An, Y. Jin, J. Li, W. Li, W. Wu, "Impact of particulate air pollution on Cardiovascular health," *Current Allergy Asthma Reports*, vol. 18, no. 15, pp. 1-6, 2018.

[3] P. M. Barros, E. H. Tanabe, M. L. Aguiar, "Performance of fibrous filters during nanoparticle cake formation," *Separation Science and Technology*, vol. 51, no. 6, pp. 1042–1052, 2016.

[4] A. Hirst, G. Evans, S. R. Larson, S. Lord, R. K. Powis, R. Stearne. Guidance for Occupational Hygienists on the Assessment and Control of the Health Risks from Metalworking Fluid (MWF). 1st Ed. England: British Occupational Hygiene Society, 2025.

[5] K. Arrhenius, A. Fischer, O. Büker, H. Adrien, A. E. Masri, F. Lestremau, et al., "Analytical methods for the determination of oil carryover from CNG/biomethane refueling stations recovered in a solvent," *RSC Advances*, vol. 10, no. 20, pp. 11907-11917, 2020.

[6] A. T. Simpson, "Comparison of methods for the measurement of mist and vapor from light mineral oil–based metalworking fluids," *Applied Occupational and Environmental Hygiene*, vol. 18, no. 11, pp. 865–876, 2003.

[7] C. T. Billiet, R. M. Fielding, "A quantitative method to determine oil carryover from high efficiency coalescing filters in compressed gases under varying dynamic conditions and the interpretation of results to assist filter system design," in *International Compressor Engineering Conference*, West Lafayette, USA, 1984.

[8] W. Zhang, K. E. Thompson, A. H. Reed, L. Beenken, "Relationship between packing structure and porosity in fixed beds of equilateral cylindrical particles," *Chemical Engineering Science*, vol. 61, no. 24, pp. 8060–8074, 2006.

[9] Z. Pan, Y. Liang, M. Tang, Z. Sun, J. Hu, J. Wang, "Simulation of performance of fibrous filter media composed of cellulose and synthetic fibers," *Cellulose*, vol. 26, no. 12, pp. 7051–7065, 2019.

[10] J. A. Hubbard, J. E. Brockmann, J. Dellinger, D. A. Lucero, A. L. Sanchez, B. L. Servantes, "Fibrous filter efficiency and pressure drop in the viscous-inertial transition flow regime," *Aerosol Science and Technology*, vol. 46, no. 2, pp. 138–147, 2012.

[11] W.W. F. Leung, C.H. Hung, "Investigation on pressure drop evolution of fibrous filter operating in aerodynamic slip regime under continuous loading of sub-micron aerosols," *Separation and Purification Technology*, vol. 63, no. 3, pp. 691–700, 2008.

[12] C. Yue, Q. Zhang, Z. Zhai, "Numerical simulation of the filtration process in fibrous filters using CFD-DEM method," *Journal of Aerosol Science*, vol. 101, pp. 174–187, 2016.

[13] S. Dhaniyala, B. Y. H. Liu, "Theoretical modeling of filtration by nonuniform fibrous filters," *Aerosol Science and Technology*, vol. 34, no. 2, pp. 170–178, 2001.

[14] A. Jackiewicz, A. Podgórski, L. Gradoń, and J. Michalski, "Nanostructured media to improve the performance of fibrous filters," *KONA Powder and Particle Journal*, vol. 30, pp. 244–255, 2013.

[15] R. C. Brown. Air Filtration: an Integrated Approach to the Theory and Applications of Fibrous Filter. 1st Ed. Oxford: Pergamon Press, 1993.

[16] W. C. Hinds. Aerosol Technology: Properties, Behavior, and Measurement of Airborne Particles. 2nd Ed. Hoboken: Wiley, 2012.

[17] A. P. Piotrowski, J. J. Napiorkowski, "Optimizing neural networks for river flow forecasting - Evolutionary Computation methods versus the Levenberg-Marquardt approach," *Journal of Hydrology*, vol. 407, no. 1–4, pp. 12–27, 2011.

[18] M. Balcilar, A.S. Dalkilic, O. Agra, S.O. Atayilmaz, S. Wongwises, "A correlation development for predicting the pressure drop of various refrigerants during condensation and evaporation in horizontal smooth and micro-fin tubes," *International Communication in Heat Mass Transfer*, vol. 39, no. 7, pp. 937–944, 2012.

[19] I. P. Beckman, G. Berry, J. Ross, G. Riveros, H. Cho, "Prediction of air filtration efficiency and airflow resistance of air filter media using convolutional neural networks and synthetic data derived from simulated media," *Journal of Aerosol Science*, vol. 171, p. 106164, 2023.

[20] A. Rostami, A. Hemmati-Sarapardeh, S. Shamshirband, "Rigorous prognostication of natural gas viscosity: Smart modeling and comparative study," *Fuel*, vol. 222, pp. 766–778, 2018.

[21] C. G. Williams, O. O. Ojuri, "Predictive modelling of soils' hydraulic conductivity using artificial neural network and multiple linear regression," *SN Applied Science*, vol. 3, no. 2, pp. 1–13, 2021.

[22] W. J. Niu, Z. K. Feng, B. F. Feng, Y. W. Min, C. T. Cheng, J. Z. Zhou, "Comparison of multiple linear regression, artificial neural network, extreme learning machine, and support vector machine in deriving operation rule of hydropower reservoir," *Water*, vol. 11, no. 1, p. 88, 2019.

[23] F. Faraji, J. O. Ugwu, P. L. Chong, F. Nabhani, "Modelling viscosity of liquid dropout near wellbore region in gas condensate reservoirs using modern numerical approaches," *Journal of Petroleum Science and Engineering*, vol. 185, pp. 1–14, 2020.

[24] F. Faraji, J. O. Ugwu, P. L. Chong, "Modelling two-phase Z factor of gas condensate reservoirs: Application of Artificial Intelligence (AI)," *Journal of Petroleum Science and Engineering*, vol. 208, pp. 1-22, 2022.

[25] F. D. Foresee, M. T. Hagan, "Gauss-newton approximation to Bayesian learning," in *Proceedings of International Conference on Neural Networks (ICNN'97)*, pp. 1930–1935, 1997.

[26] H. P. Gavin, "The Levenburg-Marqurdt algorithm for nonlinear least squares curve-fitting problems," *Duke Univ*ersity, [Online], 2019. Available: http://people.duke.edu/~hpgavin/ce281/lm.pdf

[27] M. T. Hagan, M. B. Menhaj, "Training feedforward networks with the Marquardt algorithm," *IEEE Transactions and Neural Networks*, vol. 5, no. 6, pp. 989-993, 1994.

[28] T. Hastie, R. Tibshirani, J. Friedman. The Elements of Statistical Learning: Data Mining, Inference, and Prediction. 2nd Ed. Standford: Springer, 2009.

[29] S. S. Haykin. Neural Networks: A Comprehensive Foundation. 1st Ed. New York: Macmillan, 1994.

[30] D. J. C. Mackay, "Bayesian interpolation," *Neural Computation*, vol. 4, no. 3, pp. 415–447, 1992.

[31] P. Louridas, C. Ebert, "Machine Learning," *IEEE Software*, vol. 33, no. 5, pp. 110–115, 2016.

[32] F. Faraji, C. Santim, P. L. Chong, F. Hamad, "Two-phase flow pressure drop modelling in horizontal pipes with different diameters," *Nuclear Engineering and Design*, vol. 395, pp. 1-16, 2022.

[33] S. Haykin. Neural Networks - A Comprehensive Foundation. 3rd Ed. Singapore: Pearson, 2005.

[34] M. T. Hagan, H. B. Demuth, M. H. Beale, O. D. Jesús. Neural Network Design. 2nd Ed. United States: Amazon, 2014.

[35] A. Ebrahimi, E. Khamehchi, "A robust model for computing pressure drop in vertical multiphase flow," *Journal of Natural Gas Science and Engineering*, vol. 26, pp. 1306–1316, 2015.

[36] J. J. More, "The Levenberg-Marquardt algorithm: Implementation and theory," in *Lecture Notes in Mathematics*, pp. 105-116, 2006.

[37] F. Burden, D. Winkler, "Bayesian regularization of neural networks," in *Methods Molecular Biology*, pp. 23–42, 2008.

[38] R. Eberhart, J. Kennedy, "A new optimizer using particle swarm theory," in *Proceedings of the Sixth International Symposium on Micro Machine and Human Science*, pp. 39–43, 1995.

[39] G. Zhou, H. Moayedi, M. Bahiraei, Z. Lyu, "Employing artificial bee colony and particle swarm techniques for optimizing a neural network in prediction of heating and cooling loads of residential buildings," *Journal of Cleaner Production*, vol. 254, pp. 2-14, 2020.

[40] C. Bishop. Pattern Recognition and Machine Learning. 1st Ed. Cambridge: Springer Nature, 2006.